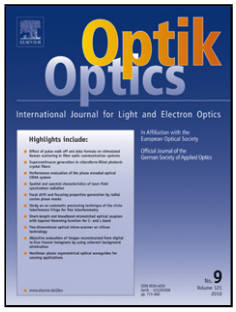

Title: Numerical Modeling Baseline for high efficiency (Cu_2FeSnS_4) CFTS based Thin Film Kesterite Solar Cell

Authors: Yousaf Hameed Khattak, Faisal Baig, Shafi Ullah, Bernabé Marí, Saira Beg, Hanif Ullah

PII: S0030-4026(18)30393-0
DOI: https://doi.org/10.1016/j.ijleo.2018.03.055
Reference: IJLEO 60644

To appear in:

Received date: 2-1-2018
Revised date: 16-3-2018
Accepted date: 16-3-2018

Please cite this article as: Khattak YH, Baig F, Ullah S, Marí B, Beg S, Ullah H, Numerical Modeling Baseline for high efficiency (Cu_2FeSnS_4) CFTS based Thin Film Kesterite Solar Cell, *Optik - International Journal for Light and Electron Optics* (2010), https://doi.org/10.1016/j.ijleo.2018.03.055

Numerical Modeling Baseline for high efficiency (Cu_2FeSnS_4) CFTS based Thin Film Kesterite Solar Cell

***Yousaf Hameed Khattak[1,2] Faisal Baig[1,2], Shafi Ullah[1], Bernabé Marí[1], Saira Beg[3], Hanif Ullah[2]**

[1] Escuela de Ingeniería de Diseño, Departamento de Física Aplicada, Universitat Politécnica de Valencia, Camí de Vera, Spain

[2]Department of Electrical Engineering, Federal Urdu University of Arts, Science and Technology Islamabad, Pakistan

[3]Department of Computer Science, COMSATS Institute of Information Technology Islamabad, Pakistan

Corresponding Author: * yousaf.hameedk@gmail.com

Abstract:

Cu_2FeSnS_4 ($CFTS$) is auspicious nontoxic and earth abundant semiconductor compound having kesterite symmetrical structure. It is an attractive and suitable material for the fabrication of low cost, high efficiency and sustainable thin film photovoltaic cell. $CFTS$ based kesterite photovoltaic cell device modeling was performed in this work. The influence of device parameters such as the thickness, acceptor and donor carrier concentration densities of absorber and electron transport layer (ETL), effect of back contact metal work function and the temperature effect on the performance of $CFTS$ based kesterite photovoltaic cell is analyzed by using one dimensional solar cell capacitance simulator (SCAPS) software. In this work, promising optimized results had been achieved with the conversion efficiency of 19.97%, fill factor (FF) 85.94 %, short-circuit current (J_{sc}) 23.37 mA/cm^2 and open circuit voltage (V_{oc}) 0.995V. The above results will give imperative baselines and feasible directions for the fabrication of higher efficiency $CFTS$ based photovoltaic cell.

Keywords: SCAPS, Photovoltaics, Cu_2FeSnS_4,$CFTS$, Kesterite, Solar cell, Numerical Analysis.

I. INTRODUCTION:

Thin film technology is the one of the most cost effective and efficient technology for the manufacturing of photovoltaic cells and it is an excellent subject of intense research in photovoltaic industry. Thin films are very suitable for low and large scale photovoltaic cell applications. To fulfill the consumer demand and for the generation of electricity, the high-power conversion efficiency solar cell without degradation of materials and economical photovoltaic cells are fabricated [1]. Silicon based photovoltaic cells dominated the market from many years and due to intensification in manufacturing capabilities thin film photovoltaic cells are gaining significance [2]. For the manufacturing and production of silicon based thin film solar cell, different major deposition techniques like sputtering, thermal evaporation, molecular beam epitaxy, e-beam evaporation, close space sublimation, and metal organic chemical vapor deposition techniques are attempted [3]. So, cost of the material, technology and energy consumption used by these sophisticated fabrication techniques makes the solar cell panel costly[4]. $CdTe$, $CIGS$ ($CuIn_{1-x}Ga_xSe_2$) and related alloy based thin-film chalcopyrite photovoltaic cells materials are commercially used for the fabrication of thin film photovoltaic devices because of high conversion efficiency, excellent electrical as well as optical properties [5] and also these types of devices have high absorption coefficient[6],[7]. The toxic materials restrict the further development of these types of cells and the rare materials like Indium and Gallium used for the fabrication of cell also increase the fabrication cost [5]. So, the commercial production of $CIGS$ based photovoltaic cell is limited.

Non-toxic earth abundant materials having kesterite symmetrical structure like $CZTS$ (Cu_2ZnSnS_4), $CZTSe$ ($Cu_2ZnSnSe_4$),[8–12] $CFTS$ (Cu_2FeSnS_4), $CFTSe$ ($Cu_2FeSnSe_4$) and their alloys are emerging as the most auspicious replacement for the chalcopyrite absorbers ($CIGS, CIGSe$) [13–15]. The growing attention towards these quaternary compounds for photovoltaic cells production is due to their potential [16–19]. Among these quaternary compounds, $CFTS$ is one of the most auspicious compound for an effective light absorber material due to its suitable optical band gap of 1.2 –1.5eV [20–24] and large absorption coefficient $\alpha > 10^4 cm^{-1}$[18,25–29]. Power conversion efficiency of about 0.29% for $CFTS$ based solar cell is presented in [30]. In [26], the reported conversion efficiency is 2.73%.

Numerical modeling or numerical analysis is an essential tool for the better understanding of device working parameters. Numerical analysis can play a significant role in manufacturing and fabrication of an efficient photovoltaic device. Numerical analysis of the kesterite based $FTO/TiO_2/CFTS/back\ contact$ photovoltaic cell is proposed in this work. In our simulations, thickness of absorber layer ($CFTS$) varies from 1µm to 4µm and the bandgap energy is $1.3eV$. The band gap of electron transport layer is larger than that of absorber layer; hence, maximum photons are absorbed in $CFTS$, which will increase the overall conversion efficiency of photovoltaic cell. The proposed results will give a valuable baseline for the design of high performance $CFTS$ based kesterite solar cells.

II. SOLAR CELL DESIGN

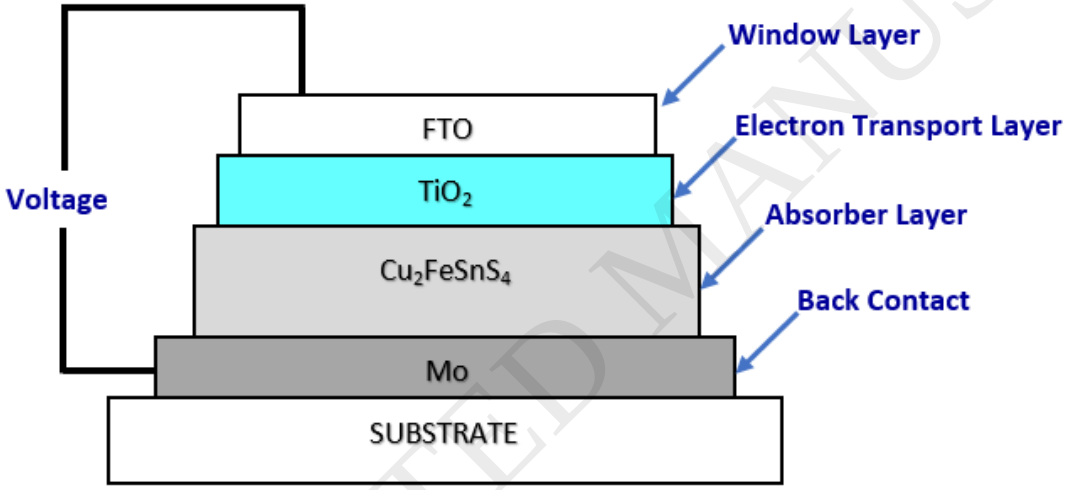

Figure 1. Block diagram of CFTS solar cell

Figure 1 shows our proposed photovoltaic cell structure $FTO/TiO_2/CFTS/Mo$, which comprises back contact layer Mo, absorber layer $CFTS$, electron transport layer TiO_2 and window layer FTO. We have investigated the influence of parameters like temperature variations, absorber layer dopant concentration and thickness, electron transport layer dopant concentration and thickness, as well as compensation ratio and illumination power of the sun, on the performance of our photovoltaic cell model. For optimum values of parameters (absorber layer thickness $4\mu m$ and acceptor carrier concentration $3 \times 10^{18}\ cm^{-3}$), we found a conversion efficiency of 19.97%.

III. NUMERICAL MODELING AND MATERIAL PARAMETERS.

The simulation software that can be used for the numerical modeling of photovoltaic cell must be able to solve the semiconductor basic equations like the continuity equation for holes and electrons and the poisson's equation relating the charge to the electrostatic potential. The charge carrier transport equation and the basic equations are well explained in simya O.K.et al [31]. We have used one dimensional Solar Cell Capacitance Simulator (SCAP-1D) software developed at the University of Gent, Belgium, to simulate our proposed model of photovoltaic cell. That software is designed for simulations and helps for analysis of J-V characteristics curve, ac characteristics (C-V and C-f), spectral response(QE) of a device, power conversion efficiency(PCE), fill factor (FF), short-circuit current (J_{sc}), open circuit

voltage (V_{oc}) used, energy bands of materials used in solar cell and concentration of different material used by solving the semiconductor basic equations, the hole and electron continuity equation and the Poissons equations.

The measure of a photovoltaic cell quality is Fill Factor (FF), which is derived by equating the maximum power (P_{max}) to the theoretical power (P_t). Where power (P_t) would be output at both the short circuit current (J_{sc}) and open circuit voltage (V_{oc}) as given in equation 1.

$$FF = \frac{P_{max}}{P_t} = \frac{V_{max}\, I_{max}}{V_{OC}\, J_{SC}} \tag{1}$$

The product of P_t and FF, divided by the energy input from the sun is the power conversion efficiency(PCE) mathematically expressed in equation 2.

$$PCE = \frac{V_{OC}\, J_{SC}\, FF}{P_{in}} \tag{2}$$

The parameters used in SCAPS software for numerical analysis are absorber layer thickness, electron-hole mobility, intrinsic carrier concentration, electron affinity, band gap and doping density. For buffer and window layer similar parameters are also required which are enlisted in table 1. Where p is the hole concentration and n is electron concentration in cm^{-3}, W is the thickness in μm. χ is the affinity in eV, E_g is the bandgap in eV, μe is the electron mobility in cm^2/Vs, μ_p is the hole mobility in cm^2/Vs, N_V is the valence band effective density of state and N_C is the conduction band effective density of states in cm^{-3}. All the simulations are performed under AM 1.5 illumination.

Table-I: Baseline parameters for modeling CFTS based solar cells[3,32,33]

Parameters	***p-CFTS***	***n*-TiO_2**	***n-FTO***
Thickness, W (μm)	*1~4*	*0.4*	*0.5*
Band gap, Eg (eV)	*1.3*	*3.2*	*3.5*
Electron affinity, χ (eV)	*3.3*	*3.86*	*4*
Dielectric permittivity, ε_r	9	9	*9*
Effective Density of states, NC (cm^{-3})	*$2.2x10^{18}$*	*$1.8x10^{19}$*	*$1x10^{19}$*
Effective Density of states, NV (cm^{-3})	*$1.8x10^{19}$*	*$2.4x10^{18}$*	*$1x10^{18}$*
Electron mobility, μ_e(cm^2/Vs)	*$2.198x10^{1}$*	*100*	*20*
Hole mobility, μ_p (cm^2/Vs)	*$2.198x10^{1}$*	25	*10*
Electron and hole concentration, n, p (cm^{-3})	*$3x10^{18}$*	*$1x10^{15}$*	*$1x10^{18}$*

IV. RESULTS AND DISCUSSION

A. Energy Band Diagram

Energy band diagram of a proposed $CFTS/TiO_2$ device is shown in figure 2 and is taken from SCAPS software. Energy band diagram helps in explaining the properties of solar cell. For incident light photons the band gap value that is optimal for most of light to be absorbed for effective power conversion efficiency is greater or equal to the maximum band gap value of 1.3 *eV*.

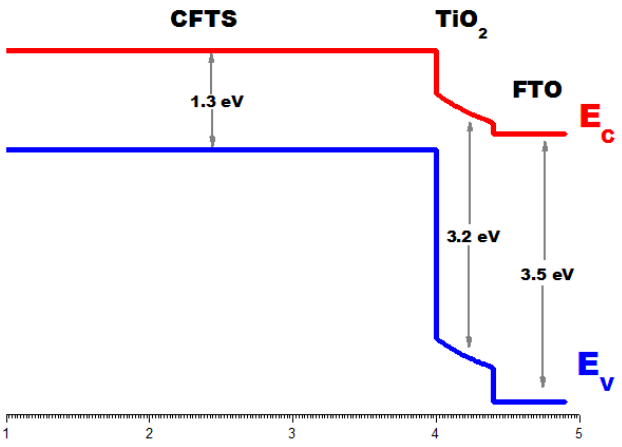

Figure 2. Energy band illustration of CFTS solar cell

B. J-V characteristics of $CFTS/TiO_2$ photovoltaic cell

The main working of a photovoltaic cell is to convert sun light energy into electricity. When there is absence of light, the photovoltaic cell is a large flat diode and gives the exponential curve in $J-V$ measurements. The cell gives an extreme smallest value of current that is due to minority carriers in dark condition, as illustrated in figure 3.

Photovoltaic cell starts working under light illumination condition. Generation of charge carriers due to absorption of incident photons from sun light in this state is the main reason of the flow of a the current. The *J-V* characteristic curve of $CFTS/TiO_2$ photovoltaic cell is given in figure 3.

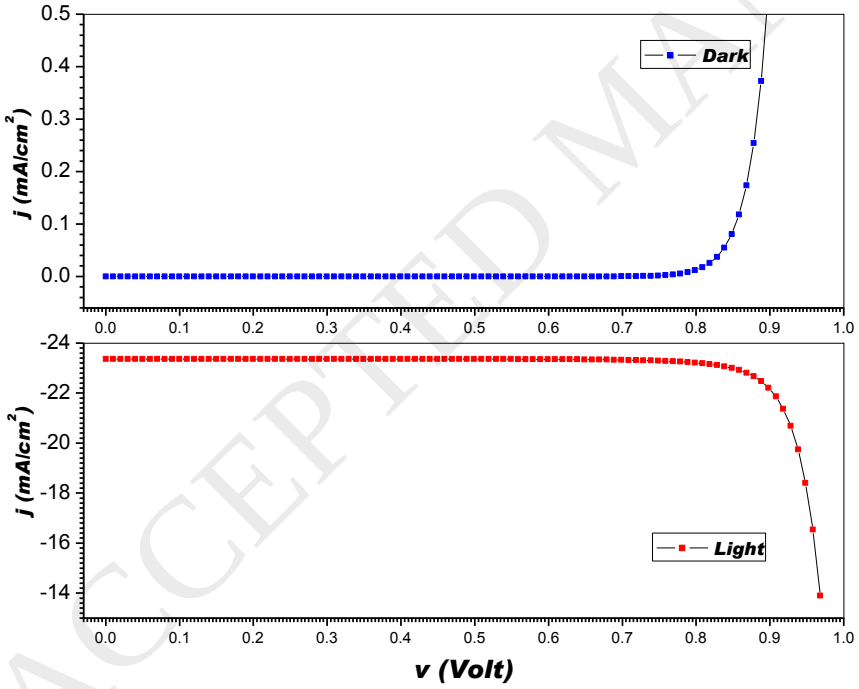

Figure 3: Dark Vs Light $J-V$ characteristics.

C. Effect of CFTS absorber layer thickness.

The absorber layer ($CFTS$) thickness effect on photovoltaic cell performance is shown in figure 4. Effect of the thickness of $CFTS$ absorber layer is analyzed by varying the thickness value from $1\mu m$ - $10\mu m$, while all other material parameters of different layers are constant. With increasing the absorber thickness, short circuit current (J_{SC}) increases with an increase of open circuit voltage (V_{OC}). Fill factor (FF) and power conversion efficiency *(PCE) are* also increases up to a point of optimal thickness. After reaching to the optimal absorber thickness values, Fill factor starts to decrease. The increase in J_{SC} with an increase of V_{OC} and PCE up to optimal absorber thickness, is principally due to

more absorption of photons of longer wavelength and this will in turn, affect the ratio of photo-generated carriers. The optimal value for absorber thickness layer is $4\mu m$.

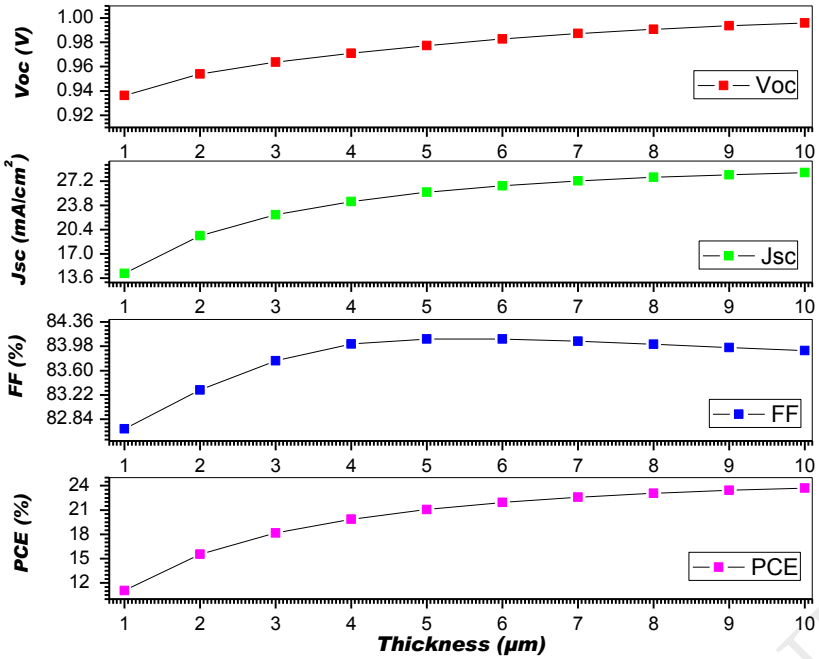

Figure 4: Effect of the absorber layer thickness on CFTS photovoltaic cells

D. Effect of absorber layer acceptor concentration densities

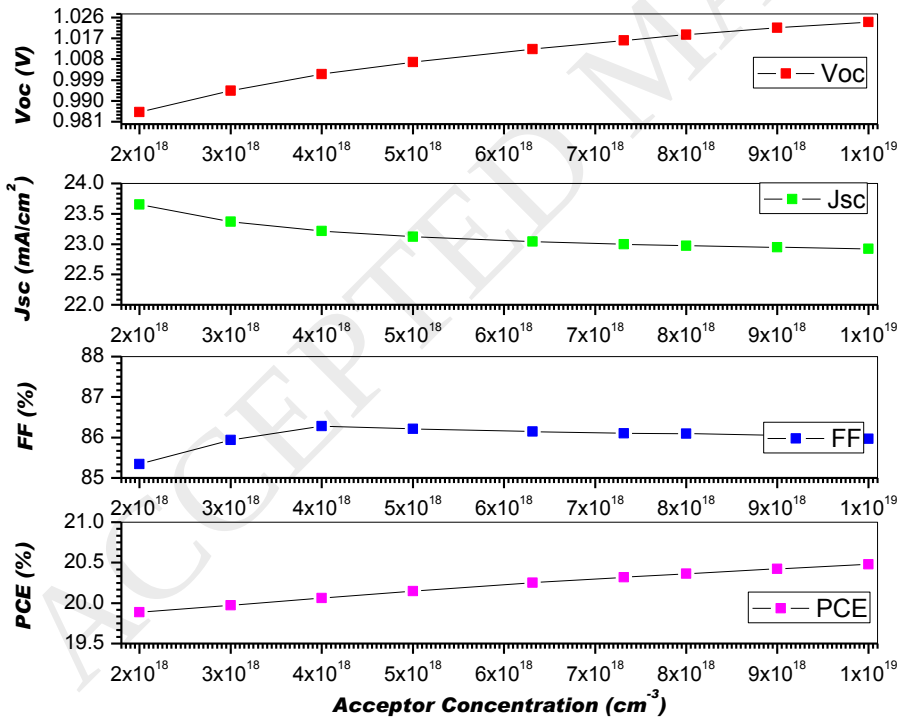

Figure 5: Acceptor concentration in the absorber layer.

Acceptor concentration densities in absorber layer is varied from $1 \times 10^{18} cm^{-3}$ to $1 \times 10^{19} cm^{-3}$ as shown in figure 5. The figure illustrates that V_{oc} increases with increase in the doping concentration whereas J_{sc} decreases with increase in the doping concentration. The main reason is that the saturation current of a device increases with the increase of the carrier concentration density and resultantly the V_{oc} increases with increasing doping concentration. However, the short-circuit current will decrease with the increasing of carrier densities. This decrease in J_{sc} with increasing doping concentration is due to the fact that the higher carrier densities will increase the recombination process and lessen the probability of the collection of the photon-generated electrons. So the collected conversion efficiency is more dependent on the influence of the concentration density. From figure 5, it is clear that power conversion effeciency and fill factor increases with increase in the carrier concentration in absorber layer material. The optimal value of the concentration of acceptor density of absorber layer is $3 \times 10^{18}\ cm^{-3}$.

E. Effect of electron transport layer on $CFTS/TiO_2$ photovoltaic cell.

TiO_2 electron transport layer(ETL) influence on the performance of a photovoltaic cell is also explored and given in figure 6. The ETL thickness is varied from $0.1\mu m$ to $1\mu m$. Simulated fallouts illustrate that with an increase in the ETL thickness, there is no change in short-circuit current (J_{sc}), open circuit voltage (V_{oc}), power conversion efficiency (PCE) and the Fill Factor (FF). So, this result is comprehended that change in thickness of ETL layer did not affect the output of $CFTS/TiO_2$ photovoltaic device. For the designing of $CFTS/TiO_2$ based kesterite device, optimum thickness taken is $0.4\mu m$.

The effect of ETL donor concentration on the deviece performance is analysed by changing the concentration density value varied from $1 \times 10^{15} cm^{-3}$ to$1 \times 10^{17} cm^{-3}$. With increase in doping concentration in ETL, there is no major change obtained that affects the performance of device as illustrated in figure 7. So, this result is comprehended that by changing the ETL donor concentration, output of photovoltaic device is not affected.

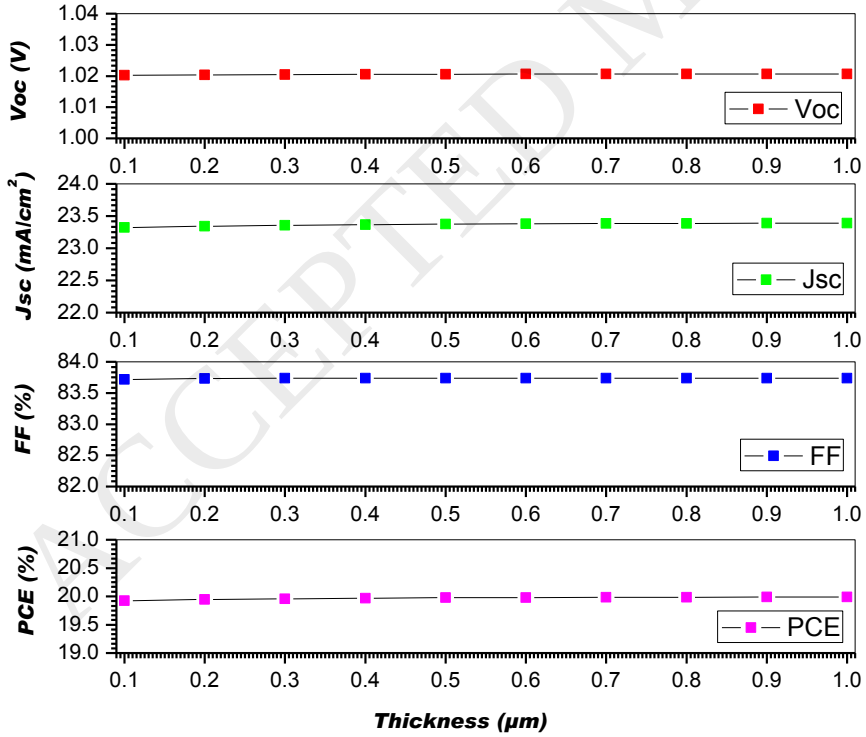

Figure 6: Effect of the Electron Transport Layer thickness on CFTS photovoltaic cells.

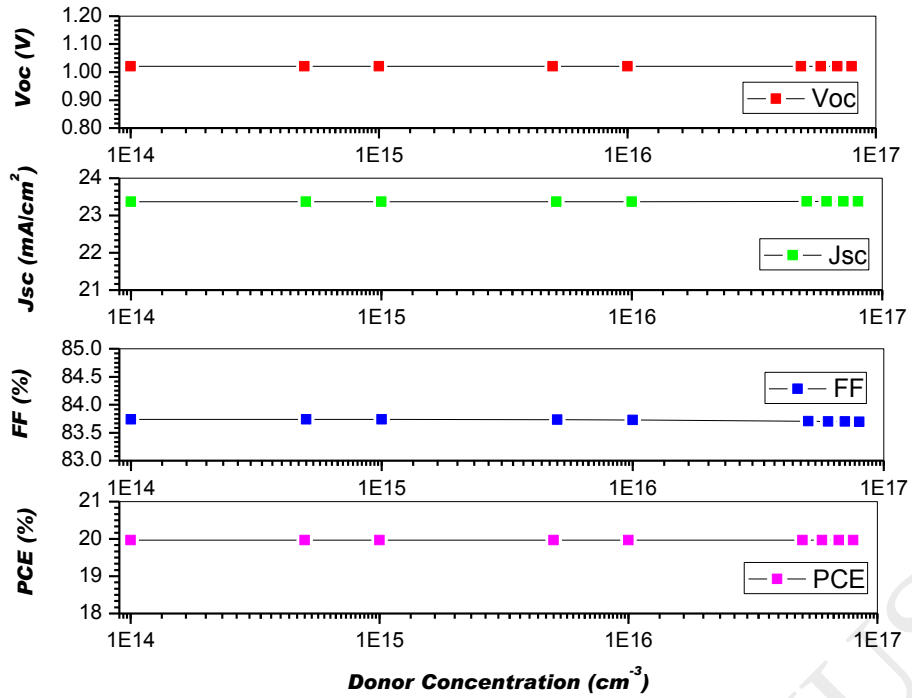

Figure 7: Donor concentration in the Electron Transport Layer.

F. Effect of back contact metal work function on JV characteristic curve.

Metal work function of back contact affects the performance of solar cell. The metal work function is well illustrated in figure 8. With increase in the contact metal work function, open circuit voltage increases. Along with open circuit voltage, short circuit current also increases. This can be explained with the aid of energy band diagram shown in figure 9 for metal work function of 4.9 eV. From figure 8, it can be seen that there is a conduction band offset which stops the flow of electrons to the back contact, thus helps in improving the open circuit voltage of solar cell.

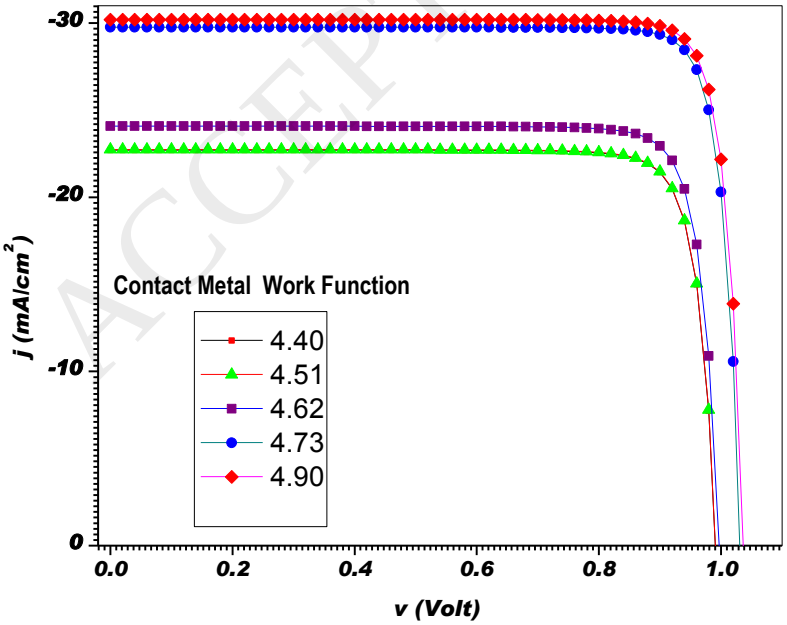

Figure 8: Effect of back contact metal work function on JV characteristic curve.

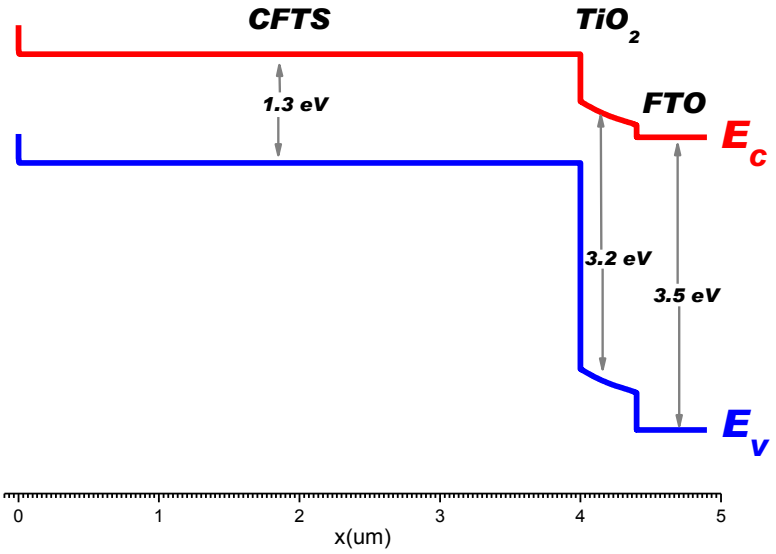

Figure 9: Energy band diagram illustration of back contact metal work function effect

G. *Effect of working temperature on photovoltaic cell performance.*

Analysis of device by means of its working temperature is explored to check the performance of photovoltaic cell. The photovoltaic panels are installed in the open sky. So, heating on photovoltaic cell increases due to the sunlight, which directly affects the performance of photovoltaic cells. The panels are operated at temperatures greater than $300K$. The influence of the working temperature on the proposed device is also investigated. For inquiring the temperature effect, we take the temperature in a rage from $300K$ to $500K$. The simulation results are shown in figure 10.

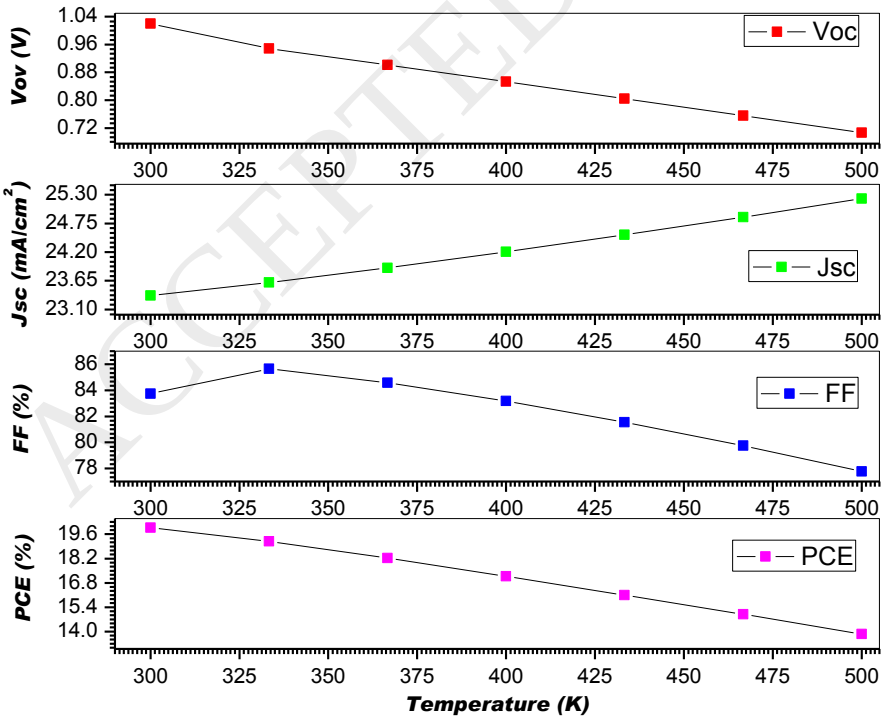

Figure 10: Effect of temperature on CFTS solar cell.

Overall solar cell performance is affected due to increase in temperature as well understood from figure 10. Power conversion efficiency and open circuit voltage decreases with increase in temperature. This decrease in conversion efficiency is due to higher temperature, because carrier concentration, band gaps, electron and hole mobility are directly affected by temperature [23]. Reverse saturation current J_0 depends on the temperature due to this V_{oc} decreases with increase in temperature as given in equation. 3[34]. Electrons gain more energy from the increased operating temperature. These electrons are unstable due to the higher temperature and are more likely to recombine with the holes before reaching the depletion region. Figure 10 illustrates that conversion efficiency, FF and V_{oc} of the device decreases; whereas J_{sc} increases with increase in temperature.

$$J_e(V) = J_0 \left[exp\left(\frac{qV_{oc}}{k_B T}\right) - 1 \right] \quad (3)$$

V. CONCLUSION:

The base line parameters of kesterite based FTO/TiO_2 / $CFTS/$ Mo photovoltaic device is proposed in this work. This will be very helpful for designers, researchers and engineers for analyzing and manufacturing of $CFTS$ based devices. The different parameters which affects the cell performance are described. For the in depth understanding and getting the confidence in the modeling of a photovoltaic cell, different characteristics, as well as different possible conditions, are to be considered for simulation. In this work, promising optimized results have been achieved with the conversion efficiency of 19.97%, fill factor (FF) 85.94 %, short-circuit current (J_{sc}) 23.37 mA/cm^2 and open circuit voltage (V_{oc}) 0.995V. The results will give imperative guidance for the feasible fabrication of higher efficiency $CFTS$ based photovoltaic cells.

ACKNOWLEDGMENTS

This work was supported by Ministerio de Economía y Competitividad (ENE2016-77798-C4-2-R) and Generalitat valenciana (Prometeus 2014/044).

REFERENCES:

[1] K. Jimbo, R. Kimura, T. Kamimura, S. Yamada, W.S. Maw, H. Araki, K. Oishi, H. Katagiri, Cu2ZnSnS4-type thin film solar cells using abundant materials, Thin Solid Films. 515 (2007) 5997–5999. doi:10.1016/j.tsf.2006.12.103.

[2] S. Hegedus, Thin film solar modules: the low cost, high throughput and versatile alternative to Si wafers, Prog. Photovoltaics Res. Appl. 14 (2006) 393–411. doi:10.1002/pip.704.

[3] H.W. Shuo Wang, Ruixin Ma, Chengyan Wangb, Shina Li, Fabrication and photoelectric properties of Cu2FeSnS4(CFTS) and Cu2FeSn(S,Se)4(CFTSSe) thin film, Appl. Surf. Sci. 422 (2017) 39–45. doi:10.1016/j.apsusc.2017.05.244.

[4] A. Mutalikdesai, S.K. Ramasesha, Solution process for fabrication of thin film CdS/CdTe photovoltaic cell for building integration, Thin Solid Films. 632 (2017) 73–78. doi:10.1016/j.tsf.2017.04.036.

[5] J. Zhou, Z. Ye, Y. Wang, Q. Yi, J. Wen, Solar cell material Cu2FeSnS4 nanoparticles synthesized via a facile liquid re fl ux method, Mater. Lett. 140 (2015) 119–122. doi:10.1016/j.matlet.2014.11.004.

[6] M.A. Green, K. Emery, Y. Hishikawa, W. Warta, E.D. Dunlop, Solar cell efficiency tables (Version 45), Prog. Photovoltaics Res. Appl. 23 (2015) 1–9. doi:10.1002/pip.2573.

[7] N. Amin, M.I. Hossain, P. Chelvanathan, A.S.M. Mukter Uzzaman, K. Sopian, Prospects of Cu2ZnSnS4(CZTS) solar cells from numerical analysis, in: Int. Conf. Electr. Comput. Eng. (ICECE 2010), IEEE, 2010: pp. 730–733. doi:10.1109/ICELCE.2010.5700796.

[8] A.D. Adewoyin, M.A. Olopade, M. Chendo, Enhancement of the conversion efficiency of Cu2ZnSnS4 thin film solar cell through the optimization of some device parameters, Opt. - Int. J. Light Electron Opt. 133 (2017) 122–131. doi:10.1016/j.ijleo.2017.01.008.

[9] F.Z. Boutebakh, M.L. Zeggar, N. Attaf, M.S. Aida, Electrical properties and back contact study of CZTS/ZnS heterojunction, Opt. - Int. J. Light Electron Opt. 144 (2017) 180–190. doi:10.1016/j.ijleo.2017.06.080.

[10] S. Ananthakumar, J. Ram Kumar, S. Moorthy Babu, Synthesis of Cu 2 ZnSnSe 4 hierarchical nanostructures by colloidal method, Opt. - Int. J. Light Electron Opt. 127 (2016) 10360–10365. doi:10.1016/j.ijleo.2016.08.058.

[11] M. Benchikhi, R. El Ouatib, L. Er-Rakho, S. Guillemet-Fritsch, J.J. Demai, B. Durand, Low-temperature molten salt synthesis and characterization of Cu 2 ZnSnS 4 ultrafine powders, Opt. - Int. J. Light Electron Opt. 138 (2017) 568–572. doi:10.1016/j.ijleo.2017.02.076.

[12] X. Zhou, W. Meng, C. Dong, C. Liu, Z. Qiu, J. Qi, J. Chen, M. Wang, Cu2ZnSnS4 quantum dots as effective electron acceptors for hybrid solar cells with a broad spectral response, RSC Adv. 5 (2015) 90217–90225. doi:10.1039/C5RA16898H.

[13] I.L. Repins, M.J. Romero, J. V. Li, S.-H. Wei, D. Kuciauskas, C.-S. Jiang, C. Beall, C. DeHart, J. Mann, W.-C. Hsu, G. Teeter, A. Goodrich, R. Noufi, Kesterite Successes, Ongoing Work, and Challenges: A Perspective From Vacuum Deposition, IEEE J. Photovoltaics. 3 (2013) 439–445. doi:10.1109/JPHOTOV.2012.2215842.

[14] H. Wang, Y. Liu, M. Li, H. Huang, H.M. Xu, R.J. Hong, H. Shen, Multifunctional TiO2nanowires-modified nanoparticles bilayer film for 3D dye-sensitized solar cells, Optoelectron. Adv. Mater. Rapid Commun. 4

(2010) 1166–1169. doi:10.1039/b000000x.

[15] H. Zhou, W.-C. Hsu, H.-S. Duan, B. Bob, W. Yang, T.-B. Song, C.-J. Hsu, Y. Yang, CZTS nanocrystals: a promising approach for next generation thin film photovoltaics, Energy Environ. Sci. 6 (2013) 2822. doi:10.1039/c3ee41627e.

[16] M.Y.V. X. Fontané , V. Izquierdo-Roca, E. Saucedo, S. Schorr, V.O. Yukhymchuk, J.R.M. A. Pérez-Rodríguez, Vibrational properties of stannite and kesterite type compounds : Raman scattering analysis of Cu2(Fe,Zn)SnS 4, J. Alloy. Compd. J. 539 (2012) 190–194. doi:10.1016/j.jallcom.2012.06.042.

[17] C. Yan, C. Huang, J. Yang, F. Liu, J. Liu, Y. Lai, Synthesis and characterizations of quaternary Cu2FeSnS4 nanocrystals, Chem. Commun. (2012) 2603–2605. doi:10.1039/c2cc16972j.

[18] B.L. and A.G. Xiaoyan Zhang, Ningzhong Bao, Karthik Ramasamy, Yu-Hsiang A. Wang, Yifeng Wang, Crystal phase-controlled synthesis of Cu2FeSnS4 nanocrystals with a band gap of around 1.5 eV, Chem. Commun. 48 (2012) 4956–4958. doi:10.1039/c2cc31648j.

[19] S.U. Schorr, H.A.-J.O. Hoebler, M.I. Tovar, A neutron diffraction study of the stannite-kesterite solid solution series, Eur. J. Mineral. 19 (2007) 65–73. doi:10.1127/0935-1221/2007/0019-0065.

[20] C. Dong, G.Y. Ashebir, J. Qi, J. Chen, Z. Wan, W. Chen, M. Wang, Solution-processed Cu 2 FeSnS 4 thin films for photovoltaic application, Mater. Lett. 214 (2018) 287–289. doi:10.1016/j.matlet.2017.12.032.

[21] Y. Liu, M. Hao, J. Yang, L. Jiang, C. Yan, C. Huang, D. Tang, F. Liu, Y. Liu, Colloidal synthesis of Cu2FeSnSe4 nanocrystals for solar energy conversion, Mater. Lett. 136 (2014) 306–309. doi:10.1016/j.matlet.2014.08.072.

[22] X. Meng, H. Deng, J. He, L. Sun, P. Yang, J. Chu, Synthesis , structure , optics and electrical properties of Cu2FeSnS4 thin film by sputtering metallic precursor combined with rapid thermal annealing sulfurization process, Mater. Lett. 151 (2015) 61–63. doi:10.1016/j.matlet.2015.03.046.

[23] X. Meng, H. Deng, J. Tao, H. Cao, X. Li, L. Sun, P. Yang, J. Chu, Heating rate tuning in structure, morphology and electricity properties of Cu2FeSnS4 thin films prepared by sulfurization of metallic precursors, J. Alloys Compd. 680 (2016) 446–451. doi:10.1016/j.jallcom.2016.04.166.

[24] R.R. Prabhakar, N. Huu Loc, M.H. Kumar, P.P. Boix, S. Juan, R.A. John, S.K. Batabyal, L.H. Wong, Facile water-based spray pyrolysis of earth-abundant Cu2FeSnS4 thin films as an efficient counter electrode in dye-sensitized solar cells, ACS Appl. Mater. Interfaces. 6 (2014) 17661–17667. doi:10.1021/am503888v.

[25] P. Nazari, A. Yazdani, Z. Shadrokh, B.A. Nejand, N. Farahani, R. Sei, Journal of Physics and Chemistry of Solids Band gap engineering of Cu3 FexS (1-x)S4 : A potential absorber material for solar energy, J. Phys. Chem. Solids. 111 (2017) 110–114. doi:10.1016/j.jpcs.2017.07.005.

[26] D.B. Khadka, J. Kim, Structural Transition and Band Gap Tuning of Cu 2 (Zn,Fe)SnS 4 Chalcogenide for Photovoltaic Application, J. Phys. Chem. C. 118 (2014) 14227–14237. doi:10.1021/jp503678h.

[27] H. Guan, H. Shen, B. Jiao, X. Wang, Structural and optical properties of Cu2FeSnS4 thin film synthesized via a simple chemical method, Mater. Sci. Semicond. Process. 25 (2014) 159–162. doi:10.1016/j.mssp.2013.10.021.

[28] M. Adelifard, Preparation and characterization of Cu2FeSnS4 quaternary semiconductor thin films via the

spray pyrolysis technique for photovoltaic applications, J. Anal. Appl. Pyrolysis. 122 (2016) 209–215. doi:10.1016/j.jaap.2016.09.022.

[29] X. Jiang, W. Xu, R. Tan, W. Song, J. Chen, Solvothermal synthesis of highly crystallized quaternary chalcogenide Cu2FeSnS4 particles, Mater. Lett. 102–103 (2013) 39–42. doi:10.1016/j.matlet.2013.03.102.

[30] C. Dong, W. Meng, J. Qi, M. Wang, Cu2FeSnS4 nanocrystals as effective electron acceptors for hybrid solar cells, Mater. Lett. 189 (2017) 104–106. doi:10.1016/j.matlet.2016.11.090.

[31] O.K. Simya, A. Mahaboobbatcha, K. Balachander, A comparative study on the performance of Kesterite based thin film solar cells using SCAPS simulation program, Superlattices Microstruct. 82 (2015) 248–261. doi:10.1016/j.spmi.2015.02.020.

[32] R.T. and G.U. Anima Ghosh, Dhirendra K. Chaudhary, Amrita Biswas, Solution-processed Cu2XSnS4 (X=Fe,Co Ni) photo-electrochemical and thin film solar cells on vertically grown ZnO nanorod arrays, RSC Adv. 6 (2016) 115204–115212. doi:10.1039/C6RA24149B.

[33] H. Hou, H. Guan, L. Li, Synthesis of Cu2FeSnS4 thin films with stannite and wurtzite structure directly on glass substrates via the solvothermal method, J. Mater. Sci. Mater. Electron. 28 (2017) 7745–7748. doi:10.1007/s10854-017-6469-6.

[34] W.E.I. Sha, X. Ren, L. Chen, W.C.H. Choy, The efficiency limit of CH 3 NH 3 PbI 3 perovskite solar cells, Appl. Phys. Lett. 106 (2015) 221104. doi:10.1063/1.4922150.